A Novel Mutant Cardiac Troponin C Disrupts Molecular Motions Critical for Calcium Binding Affinity and Cardiomyocyte Contractility

Chee Chew Lim,*† Haijun Yang,§ Mingfeng Yang,§ Chien-Kao Wang,¶ Jianru Shi,‡‡ Eric A. Berg,‡ David R. Pimentel,† Judith K. Gwathmey,‖ Roger J. Hajjar,** Michiel Helmes,†† Catherine E. Costello,‡ Shuanghong Huo,§ and Ronglih Liao‡‡

*Department of Cardiovascular Medicine, Vanderbilt University School of Medicine, Nashville, Tennessee; Department of †Medicine and ‡Biochemistry, Boston University School of Medicine, Boston, Massachusetts; §Gustaf H. Carlson School of Chemistry and Biochemistry, Clark University, Worcester, Massachusetts; ¶Departments of Physiology and Biophysics, University of Washington, Seattle, Washington; ‖Gwathmey Inc., Cambridge, Massachusetts; **Massachusetts General Hospital and Harvard Medical School, Cardiovascular Research Center, Charlestown, Massachusetts; ††IonOptix Europe, Wageningen, the Netherlands; and ‡‡Cardiovascular Division, Brigham and Women's Hospital and Harvard Medical School, Boston, Massachusetts

ABSTRACT Troponin C (TnC) belongs to the superfamily of EF-hand (helix–loop–helix) Ca^{2+}-binding proteins and is an essential component of the regulatory thin filament complex. In a patient diagnosed with idiopathic dilated cardiomyopathy, we identified two novel missense mutations localized in the regulatory Ca^{2+}-binding Site II of TnC, $TnC^{(E59D,D75Y)}$. Expression of recombinant $TnC^{(E59D,D75Y)}$ in isolated rat cardiomyocytes induced a marked decrease in contractility despite normal intracellular calcium homeostasis in intact cardiomyocytes and resulted in impaired myofilament calcium responsiveness in Triton-permeabilized cardiomyocytes. Expression of the individual mutants in cardiomyocytes showed that TnC^{D75Y} was able to recapitulate the $TnC^{(E59D,D75Y)}$ phenotype, whereas TnC^{E59D} was functionally benign. Force-pCa relationships in $TnC^{(E59D,D75Y)}$ reconstituted rabbit psoas fibers and fluorescence spectroscopy of $TnC^{(E59D,D75Y)}$ labeled with 2-[(4′-iodoacetamide)-aniline]-naphthalene-6-sulfonic acid showed a decrease in myofilament Ca^{2+} sensitivity and Ca^{2+} binding affinity, respectively. Furthermore, computational analysis of TnC showed the Ca^{2+}-binding pocket as an active region of concerted motions, which are decreased markedly by mutation D75Y. We conclude that D75Y interferes with proper concerted motions within the regulatory Ca^{2+}-binding pocket of TnC that hinders the relay of the thin filament calcium signal, thereby providing a primary stimulus for impaired cardiomyocyte contractility. This in turn may trigger pathways leading to aberrant ventricular remodeling and ultimately a dilated cardiomyopathy phenotype.

INTRODUCTION

The thin filament proteins, the troponins and tropomyosin, are the regulatory elements that coordinate striated muscle contraction (1,2). The troponin complex is composed of three structurally and functionally distinct subunits: troponin C (TnC) is the calcium binding subunit, troponin T (TnT) anchors the troponin complex to tropomyosin, and troponin I (TnI) together with tropomyosin regulate accessibility of the myosin binding sites on actin. During systole, binding of calcium to the regulatory domain of TnC is the critical first step that elicits a series of conformational changes in the troponin complex to weaken the inhibitory action of TnI and tropomyosin. This enables the myosin heads to bind to actin and generate force. Cardiac and skeletal TnC both contain four EF-hand or helix–loop–helix Ca^{2+}-binding motifs and are numbered I–IV, although Site I at the N-terminus of cardiac TnC (cNTnC) has been rendered inactive due to nucleotide substitutions in the cardiac TnC gene (3). Binding Sites III and IV at the C terminus of TnC are high affinity Ca^{2+}/Mg^{2+} binding sites and are always occupied by either divalent cation under normal physiological conditions (4,5), and are thought to play a role in TnC-TnI interaction (6). It is Site II at cNTnC that acts as a Ca^{2+}-sensitive molecular switch that on binding of calcium and subsequent interaction with TnI induces a conformational change in cNTnC from the 'closed' to 'open' state that serves to propagate the signal along the thin filaments to release inhibition, allowing actin-myosin interaction to occur (7,8). Given the crucial role of TnC in sensing intracellular calcium levels and triggering the cardiac contractile cycle, it is not surprising that cardiac TnC is among the most highly conserved genes in vertebrate species (9).

Using molecular cloning and DNA sequencing techniques, we identified two novel missense mutations, E59D and D75Y, in cardiac TnC isolated from a patient diagnosed with idiopathic dilated cardiomyopathy (IDCM), a disease of unknown etiology characterized by ventricular dilatation and contractile dysfunction. To our knowledge, these are the first mutations identified in cardiac TnC that are localized in regulatory Ca^{2+}-binding Site II. Binding of calcium in EF-hand II of the 12 amino acid residue-loop involves six negatively charged residues, localized in positions 1 ($+x$), 3 ($+y$), 5 ($+z$), 7 ($-y$), 9 ($-x$), and 12 ($-z$) (3,10). Mutation

Submitted May 15, 2007, and accepted for publication November 2, 2007.

Address reprint requests to Chee Chew Lim, PhD, Department of Cardiovascular Medicine, Vanderbilt University School of Medicine, 2220 Pierce Ave, PRB 359B, Nashville, TN 37232. Tel.: 615-936-2510; Fax: 615-936-1872, E-mail: chee.lim@vanderbilt.edu; or to Shuanghong Huo, PhD, Gustaf H. Carlson School of Chemistry and Biochemistry, Sackler Science Building, Rm. N200B, Clark University, 950 Main Street, Worcester, MA 01610. Tel: 508-793-7533, Fax: 508-793-8861, E-Mail: shuo@clarku.edu.

Editor: Cristobal G. dos Remedios.

0006-3495/08/05/3577/13 $2.00

doi: 10.1529/biophysj.107.112896

D75Y, in particular, is located adjacent to the $-z$ coordinate and could potentially interfere with normal calcium binding and/or signal transduction.

In an effort to elucidate the functional relevance of the missense mutations in the regulatory Ca^{2+}-binding domain of TnC we adopted a systematic approach that combines targeted expression/integration of recombinant mutant TnC in cardiomyocytes and in vitro functional assessment, with protein chemistry and computational analysis of the mutant TnC structure. Adenoviral expression of recombinant $TnC^{(E59D,D75Y)}$ in rat cardiomyocytes showed impaired cell contractility (despite normal calcium homeostasis) and a decrease in myofilament calcium responsiveness in electrically stimulated intact cells and triton-permeabilized cells, respectively. The functional $TnC^{(E59D,D75Y)}$ phenotype was recapitulated with cells expressing recombinant TnC^{D75Y}, but not TnC^{E59D}. Force-pCa relationships in rabbit psoas fibers reconstituted with mutant $TnC^{(E59D,D75Y)}$ and fluorescence spectroscopy of IAANS-labeled $TnC^{(E59D,D75Y)}$ showed a decrease in myofilament Ca^{2+}-sensitivity and Ca^{2+}-binding affinity, respectively. Interestingly, normal mode analysis of the Ca^{2+}-free form of TnC showed Ca^{2+}-binding Site II as an active area of dynamic concerted motions that is markedly reduced in the TnC^{D75Y} mutant. Our study provides mechanistic insight into how a specific mutation in the regulatory domain of TnC might alter calcium binding and signal transmission with consequent myocyte contractile dysfunction.

MATERIALS AND METHODS

Identification of two missense mutations in cardiac TnC

Total RNA was isolated from ~1 g of left ventricular tissue, isolated from a patient diagnosed with IDCM, by the guanidium isothiocyanate method (11). First strand cDNA was synthesized using AMV reverse transcriptase (Invitrogen, Carlsbad, CA). A pair of oligonucleotide primers for synthesis of the double-strand cDNA encoding human TnC were constructed according to the published cDNA sequence (12). The product of the first strand cDNA reaction was then directly used in a PCR (polymerase chain reaction) with the synthesized primer pair in the presence of *Taq* DNA polymerase. PCR products were purified using 1% low melting point (LMP) agarose gel (Gibco-BRL, Rockville, MD). The purified PCR products were cloned into a TA cloning vector pCR 2.1 (Invitrogen) followed by the standard procedures for transformation and propagation of the recombinant molecules in an *Escherichia coli* host. The recombinant DNA molecules were then purified and digested by the selected restriction enzymes. The digested cDNA was again purified by LMP gel and subcloned into a pET-24 expression vector (Novagen, La Jolla, CA) for sequence analyses. Sequenase Version 2.0 DNA Sequencing Kit (USB, Cleveland, OH) was used to carry out DNA sequence analysis. This procedure was repeated multiple times using different tissue sections from the same heart, with the same result.

Mutagenesis and generation of recombinant adenovirus

Human TnC (WT) cDNA was subcloned into pGEM vector and mutagenesis was carried out by PCR (Stratagene, La Jolla, CA) using oligonucleotide 5′-AGCTGCAGGA**T**ATGATCGATG-3′ for mutation E59D and 5′-GTGGACTTT**T**ATGA GTTCC-3′ for mutation D75Y (the mutation is in bold and underlined). E59D/D75Y TnC was generated by consecutive mutations of E59D and D75Y. $TnC^{(E59D,D75Y)}$, TnC^{E59D}, TnC^{D75Y}, and WT TnC were subcloned into the pAdTrack-CMV shuttle vector using the Xba I and Sal I sites (Qbiogene, Carlsbad, CA). Each vector construct contained two independent CMV promoters, one for the cDNA insert and one for the reporter gene, green fluorescent protein (GFP). The recombinant adenovirus was generated through homologous recombination of the vector construct with the pAdEasy-1 adenoviral plasmid in *E. coli* BJ5183 cells. The recombinant products were amplified in HEK293 cells and expression levels were confirmed by GFP fluorescence and Western blot detection. The recombinant adenoviruses were further amplified to high titer in HEK293 cells, and band-purified by centrifugation in CsCl gradients to yield stock titers of $1–3 \times 10^{10}$ plaque-forming-units (pfu)/ml.

Primary cultures of adult rat ventricular myocytes

Ventricular myocytes were isolated from adult Wistar rats (200–250 g) using a collagenase-based method, as previously described (13,14). Myocytes were cultured on laminin-coated coverslips (microscopy and cell function experiments) or p100 plates (Western blots and mass spectrometry) in serum-free DMEM (Gibco-BRL) that contained in mM: 5 carnitine, 5 creatine, 10 taurine, 100 bromodeoxyuridine, 50 U/ml penicillin, and 50 μg/ml streptomycin at 37°C in 5% CO_2. After 1 h the culture medium was removed and myocytes were infected with WT TnC, mutant TnC, or lacZ adenovirus diluted in culture media at a multiplicity of infection (MOI) of 100. Myocytes not infected with virus were included as an adenoviral control. Culture media was replaced at Day 1 and again at Day 3 postinfection. Myocytes were studied at 4 days postinfection.

SDS PAGE and Western blot

At 4 days postinfection, myocytes were washed in Ca^{2+}-free solution (in mM: 10 EGTA, 5.9 MgAc, 5.9 Na_2ATP, 10 creatine phosphate, 40 imidazole, 70 K^+-propionate, 5 NaN_3, and 1 dithiothreitol). Myocytes were then permeabilized in relaxing solution containing 1% Triton X-100 at 4°C. After 50 min, the permeabilized myocytes were washed in relaxing solution, harvested, and sonicated in 40 mM Tris-HCl buffer. The samples were solubilized in sample buffer heated at 70°C for 5 min and 100 μg of protein sample was loaded onto a 12% Bis-Tris gel (Invitrogen). For Western blot analysis, proteins were transferred onto PVDF membranes after SDS-PAGE. Antibodies to TnC (1A2, Biodesign International Saco, ME), TnI and TnT (C-19 and CT3, Santa Cruz Biotechnology, Santa Cruz, CA) and tropomyosin and actin (CH1 and AC-40, Sigma, St. Louis, MO) were used. To detect GFP, intact myocytes were harvested in cell lysis solution, sonicated, and solubilized in sample buffer heated to 95°C for 5 min. Electrophoresis and transfer was carried out as above and GFP protein content was determined by immunoblot with GFP antibody (B2, Santa Cruz Biotechnology).

Mass spectrometry

Incorporation of adenoviral expressed TnC into the thin filament complex was determined by MALDI-TOF/MS, as mutant TnC could not be distinguished from endogenous rat TnC by gel electrophoresis. Myocytes were Triton-permeabilized to eliminate artifacts from unincorporated cytosolic TnC, solubilized, and subjected to SDS-PAGE (see preceding section). The gels were Coomassie-stained and the identified TnC gel band was excised, minced, washed, reduced with DTT, alkylated with iodoacetamide, and digested with AspN at pH 7.2 (15,16). The digested peptide fragments were extracted from the gel pieces and desalted using $Ziptips_{C18}$ (Millipore, Billerica, MA) according to manufacturer's instruction and analyzed using an Applied Biosystems/MDS-Sciex QStar Pulsar quadrupole/orthogonal acceleration MALDI/TOF mass spectrometer with a nanospray source. To

determine the percent of exogenous mutant TnC incorporation in rat cardiomyocytes, a dilution series of a synthesized peptide covering the mutant TnC region ($_{73}$DF**Y**EFLVMMVRCMK^{86}, mutation is underlined in bold) and the peptide corresponding to control TnC ($_{75}$DEFLVMMVRCMK^{86}) was prepared and analyzed by mass spectrometry in triplicate. Peak intensity (counts per second) and integrated peak areas in the mass spectra of multiple digested peptide fragments were compared to the integrated area of the known concentrations of synthesized peptides, to yield the percent incorporation of exogenous mutant-TnC.

Confocal fluorescence microscopy

At 4 days postinfection, myocytes on coverslips were fixed in 3% paraformaldehyde and 2% sucrose in PBS for 15 min, permeabilized in 0.2% Triton X-100 in PBS for 15 min, and blocked in 0.1% BSA in PBS for 1 h. Myocytes were incubated with a monoclonal antibody to troponin C (1A2, Biodesign International) for 1 h, washed in PBS, and incubated for 1 h with secondary antibody conjugated to Cy5 (Alexa Fluor 647, Invitrogen-Molecular Probes, Carlsbad, CA). After washing with PBS, myocytes were double immunolabeled with monoclonal α-actinin antibody (EA53, Sigma) conjugated to TRITC (Pierce, Rockford, IL). Stained preparations were mounted onto slides with antifade (SlowFade, Molecular Probes) and analyzed for TRITC, Cy5, and GFP fluorescence with a Leica TCS SP2 AOBS confocal laser scanning microscope.

Myocyte function and fura-2 fluorescence

Cell length and intracellular calcium were determined simultaneously by video-edge detection and fura-2 fluorescence, respectively, as described previously (13,14). The myocyte was perfused with 1.2 mM Ca^{2+} Tyrode solution at 37°C and electrically stimulated at a rate of 3 Hz. Adenoviral infection of the myocyte was confirmed by GFP fluorescence before data acquisition. To minimize the chance of unequal GFP expression between myocytes, the photon count due to GFP fluorescence was measured from a fixed region of interest within all myocytes. Only myocytes with a photon count in the range of ~400 from the measured area were selected for further study. After 10 min of baseline stabilization, myocyte contractility and fura-2 fluorescence were simultaneously recorded (see Fig. 3 *A*). Cell contractility was assessed by % cell shortening, which is the ratio of twitch amplitude (difference of end-diastolic and peak systolic cell lengths) to end-diastolic cell length.

Myofilament calcium responsiveness

The experimental procedure used to measure myofilament calcium responsiveness was modified from a protocol described previously (17). Briefly, coverslips with myocytes at 4 days postinfection were affixed to a perfusion chamber that was mounted on an inverted microscope (Nikon Diaphot epifluorescence microscope). The myocytes were visualized using a Nikon ×40 (1.3 numerical aperture) oil-immersion fluorescence objective lens, and imaged on a computer screen using a variable frame rate (60–240 Hz) CCD-camera, at a sampling speed of 240 Hz. Sarcomere length was determined in real-time using specialized acquisition and analysis software (IonOptix Corp., Milton, MA). A single myocyte was selected and exclusively perfused with Ca^{2+}-free Tyrode solution (in mM: 137 NaCl, 5.4 KCl, 0.5 $MgCl_2$, 10 HEPES, 10 glucose, pH 7.4). Adenoviral infection of the myocyte was confirmed by GFP fluorescence. The myocyte was permeabilized subsequently in relaxing solution (in mM: 10 EGTA, 5.9 MgAc, 5.9 Na_2ATP, 10 creatine phosphate, 40 imidazole, 70 K^+-propionate, 5 NaN_3, and 1 DTT) containing 1% Triton X-100. After myocyte permeabilization (~2 min) myocytes were perfused with relaxing solution (pCa9). After a 5-min stabilization period, the relaxing solution was switched to a new pCa solution and sarcomere length shortening continually monitored until it achieved steady state. The myocyte was reperfused subsequently with relaxing solution until slack sarcomere length was achieved (see Fig. 4 *A*). This process was repeated for the various pCa solutions. Responsiveness of the myofilaments to calcium was assessed by determining the relationship between the sarcomere length shortened to steady state and its corresponding pCa (see Fig. 4 *B*).

Expression and purification of recombinant TnC

Mutant TnC$^{(E59D,D75Y)}$ cDNA was generated from human cTnC cDNA by site-directed mutagenesis (Quickchange, Stratagene) and subcloned into pET-24a(+) (Novagen). WT or mutant cTnC constructs were transformed into *E. coli* strain BL21 (DE3) lysogen (Novagen) for isopropyl-1-thio-b-D-galactopyranoside (IPTG) induction of T7 RNA polymerase expression of the target proteins. The IPTG-induced bacterial culture was harvested by centrifugation and the pellet resuspended in a buffer solution containing 25 mM Tris, 2 mM EDTA, 8% sucrose, 0.2% Triton X-100, 100 mM PMSF, 10 mg lysozyme, at pH 8.0. The suspension was sonicated for 10 min and centrifuged at 35,000 × *g* for 1 h. The supernatant was dialyzed against an alkaline buffer (in mM: 6000 urea, 50 Tris, 1 EGTA, 3 DTT, pH 8.0) and loaded onto a DEAE-52 column (Whatman, Florham Park, NJ). Unpurified recombinant protein was eluted from the column with a linear gradient of 0–400 mM KCl, pooled and extensively dialyzed against a Ca^{2+} buffer (in mM: 50 Tris, 300 KCl, 1 DTT, 5 $CaCl_2$, at pH 7.5). The dialyzed protein was chromatographed in a phenyl-Sepharose CL 4B (Sigma) column, washed with 2 volumes of low salt Ca^{2+} buffer, and eluted from the column with an EGTA-buffer (in mM: 50 Tris, 100 KCl, 1 DTT, 20 EGTA, at pH 7.5). The purified proteins were pooled and extensively dialyzed in ddH_2O to remove salts, lyophilized, and stored at −20°C until use. Native skeletal TnC was purified from ether powder of rabbit skeletal muscle as described previously by Potter (18).

Force-pCa measurements

Single fibers from rabbit psoas muscle were isolated, chemically permeabilized in relaxing solution (see below) containing 1% Triton X-100, and the ends fixed with glutaraldehyde and wrapped with aluminum foil T-clips for mounting on a force measurement apparatus as described previously (19). Fibers were attached to a Cambridge force transducer on one end and a micromanipulator on the other, and the mechanical apparatus mounted on a stage of an inverted microscope. Sarcomere length was measured by the He-Ne laser diffraction method and set at ~2.5 μm. Solution changes were achieved by rapidly immersing the fiber in individual custom-made chambers containing various pCa activating solutions. The composition of relaxing (pCa 9.2) and Ca^{2+} activating solutions were calculated and solutions were made as described previously (19). Calcium activating solutions were made by varying the amount of $Ca(propionate)_2$ in Ca^{2+}-free relaxing solution (in mM: 3 Mg ATP, 15 phosphocreatine, 15 EGTA, 83 MOPS, 1 Mg^{2+}, 133 Na^+ + K^+, 25 U/ml creatine kinase). Ionic strength was 0.17 M and pH was 7.0 at 20°C. Extraction of endogenous skeletal TnC was achieved by treating the permeabilized fibers with an extraction solution containing trifluoperazine (in mM: 20 Tris, 5 EDTA, and 0.5 TFP, pH 7.8) for 5–12 min. SDS-PAGE analysis of myofibril extracts confirmed that TnC was affected primarily by the extraction reconstitution protocol (see Fig. 5 *A*). Endogenous skeletal TnC extraction was verified by a reduction in force at pCa 4.0 to <2% of the pre-extraction value (see Fig. 5 *B*). Native skeletal TnC or recombinant TnC was incorporated in the TnC depleted fibers by incubation in a relaxing solution containing 0.5 mg/ml TnC. Reconstitution of TnC was considered complete when force at pCa 4.0 no longer increased with subsequent incubations, typically 10 min of total incubation. Steady-state isometric force was measured at each pCa, followed by slack measurement in pCa 9.2 to obtain baseline tension (see Fig. 5 *B*). Active force was obtained by subtracting total tension at each pCa from resting tension. The relative force (F) versus pCa was determined for each experiment and a modified Hill equation fitted to the data: $F = [Ca^{2+}]^n/(K^n + [Ca^{2+}]^n)$, with pCa at half-maximal force calculated as $pCa_{50} = -\log(K)$, and n representing the slope of the force relationship (Hill coefficient), a measure of cooperative activity.

Fluorescence-pCa measurements

Fluorescent probe 2-((4′-iodoacetamido)-anilino) naphthalene-6-sulfonic acid (IAANS, Molecular Probes) was used to label cysteines 35 and 84 in the purified recombinant TnC proteins and steady-state fluorescence measurements was carried out using SPEX DM3000 fluorescence spectrometer as described previously (20). Proteins labeled with IAANS were excited at 335 nm. In the Ca^{2+} titration experiments, small aliquots of a standard $CaCl_2$ solution were added to fluorescently labeled TnC. Changes in fluorescence intensity induced by binding of Ca^{2+} to IAANS labeled TnC was monitored at the peak emission wavelength of 450 nm. Data were fitted using a modified Hill equation: $F/F_{max} = [Ca^{2+}]^n/(K^n + [Ca^{2+}]^n)$, where F is the fluorescence change at a given $[Ca^{2+}]$, F_{max} is the maximal change in fluorescence, and K is the binding constant (21). The pCa at half-maximal fluorescence (pCa_{50}) was calculated as $pCa_{50} = -\log(K)$.

Molecular dynamics simulations

Molecular dynamics (MD) simulations (6 ns) were carried out on both the WT and D75Y forms of the Ca^{2+}-free N-lobe of troponin C (PDB entry: 1SPY) (22) at neutral pH and room temperature, 300 K with the AMBER simulation package (23) and the all-atomic force field, parm99 (24). The D75Y TnC mutant was generated by substituting Asp at position 75 in the WT with Tyr using MOE (from Chemical Computing Group). The C_β coordinates of Asp75 was kept in Tyr75, as a result, Tyr75 initially pointed toward the solvent as Asp75. To keep the whole system neutral, counter ions were added for both wild-type and D75Y-mutant. The TIP3P three-site rigid water model was used to solvate the protein and counter ions (25). The system was constructed using the periodic boundary conditions consisting of the protein with 89 residues, counter ions, and water molecules that totaled up to 21,926 atoms. The MD simulations were carried out in the N, P, and T ensemble. The temperature and pressure of the system were regulated using the Berendsen coupling algorithm with a coupling constant of 1.0 ps (26). The particle mesh Ewald (PME) summation method was used to treat the long-range electrostatic interactions (27). A 9 Å cutoff was used to limit the direct space sum in PME. All bond lengths involving H atoms were constrained with the SHAKE algorithm (28). The time step was 1.5 fs. The system was minimized 1000 steps to relax the bad contacts. After that, the system was gradually heated to 300 K, and then equilibrated for 30 ps. In the production run, the snapshots were saved every 1.5 ps. With this protocol, a 6-ns production run was carried out for the wild-type and the mutant, respectively. The secondary structure analysis was carried out using DSSP (29). The van der Waals interaction energy between Tyr75 and helix N was calculated with the ANAL module in AMBER and averaged over the last 4.5 ns with an interval of 150 ps.

Normal mode analysis

Using the same starting structures as in the MD simulations, we carried out the normal mode analysis on both the wild-type and the D75Y mutant. The proteins were minimized using Newton-Raphson algorithm with distance dependent dielectric constant to mimic solvent screening. The minimization was stopped when the rms gradient was smaller than 0.00001 kcal/(mol Å). Finally, the normal mode analysis was carried out with nmode module in Amber 7 package. The cross-correlation coefficient matrix was built from the 500 lowest frequency normal modes because the high frequency modes are generally localized in proteins and therefore do not contribute to large conformational changes (30). The cross-correlation coefficient is defined as:

$$C(i,j) = \frac{\Delta\vec{r}_i \cdot \Delta\vec{r}_j}{|\Delta\vec{r}_i||\Delta\vec{r}_j|},$$

where $\Delta\vec{r}_i$ and $\Delta\vec{r}_j$ are the displacement vectors for Cα atoms of residues i and j (31). If the motions of two atoms are perfectly correlated, the cross correlation coefficient is 1, whereas -1 indicates the strongest anti-correlated motion, which is usually seen in protein unfolding.

Statistical analysis

Data are expressed as mean ± SE. Statistical analysis was carried out using GraphPad Prism 5 software. Student's t-test was used to compare mean values of WT versus $TnC^{(E59D,D75Y)}$. Group comparison was carried out using one-way analysis of variance (ANOVA) with a Newman-Keuls multiple comparison post-hoc test. Analysis by two-way ANOVA compared individual means by Bonferroni post-hoc test. A p-value of <0.05 was considered statistically significant.

RESULTS

Myofilament incorporation of exogenously expressed TnC

To assess the functional phenotype of the mutations, we expressed recombinant WT and mutant TnC in rat cardiac myocytes using standard adenoviral techniques. Myofilament proteins are incorporated stoichiometrically into the sarcomere lattice (32,33), and strong somatic TnC expression should eventually lead to replacement of endogenous TnC in the myofilaments during the process of normal protein turnover. In Fig. 1 *A*, adenoviral co-expression of lacZ, WT, or $TnC^{(E59D,D75Y)}$ with GFP at an MOI of 100 resulted in >95% transfection efficiency of rat cardiomyocytes after 4 days, as determined by X-gal staining and GFP fluorescence. Western blot analysis showed that concomitant GFP levels were similar among the three groups (Fig. 1 *A*, *lower panel*).

We used mass spectrometry to distinguish the amount of exogenously expressed TnC from endogenous TnC incorporated into the myofilaments of cardiomyocytes at 4 days postinfection. The mass spectrometry pattern yielded identifiable peptide fragments, containing the D75Y mutation ($_{73}$DFYEFLVMMVRCMK^{86}) and the endogenous rat TnC ($_{75}$DEFLVMMVRCMK^{86}). Analysis of the mass spectrometry pattern showed that 35–40% of the endogenous TnC was replaced by exogenous $TnC^{(E59D,D75Y)}$ as determined by peak intensity (33.6 ± 11.9%) and integrated area (37.6 ± 10.6%).

Mutant TnC does not alter myofilament stoichiometry nor sarcomere structure

In striated muscle, myofilament architecture is highly regulated and stoichiometry between the proteins strictly maintained. To address whether incorporation of exogenously expressed TnC resulted in altered myofilament stoichiometry, we examined myofilament protein levels in cardiomyocytes by Western blot. Cardiomyocytes infected with WT or mutant recombinant TnC adenovirus show comparable levels of thin filament proteins: actin, troponin T, tropomyosin, troponin I, and troponin C (Fig. 1 *B*). We also did not detect any differences in any of these proteins between uninfected cells and cells infected with recombinant TnC adenovirus (data not shown).

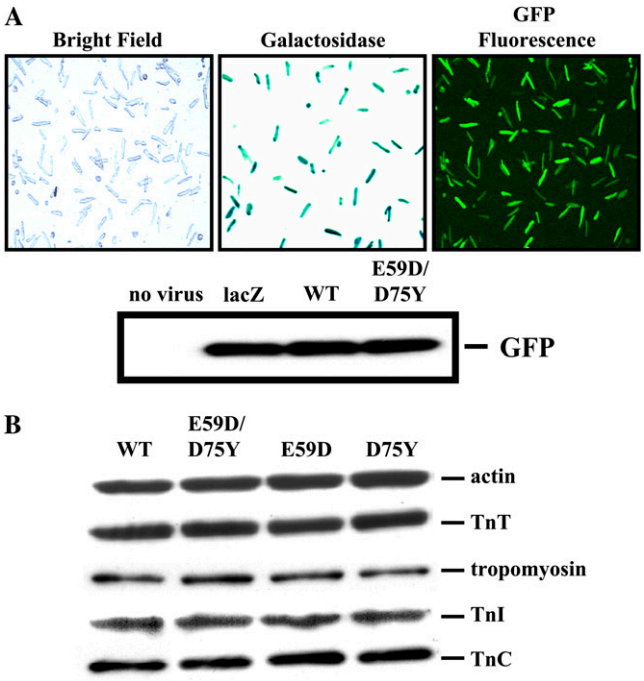

FIGURE 1 GFP and lacZ expression in adult rat ventricular myocytes at 4 days post adenoviral infection. (*A*) Bright field image of myocytes (*left*) with galactosidase staining (*middle*), and GFP fluorescence (*right*), showing robust adenoviral infection. Shown in the *lower panel* is a representative Western blot with similar expression levels of GFP in lacZ, WT, and $TnC^{(E59D,D75Y)}$ myocytes. GFP Western blot was repeated 4 times. (*B*) Western blot analysis of actin, tropomyosin, TnT, TnI, and TnC in adenoviral infected myocytes show no difference in the levels of thin filament proteins. The experiment was repeated 4 times for each antibody.

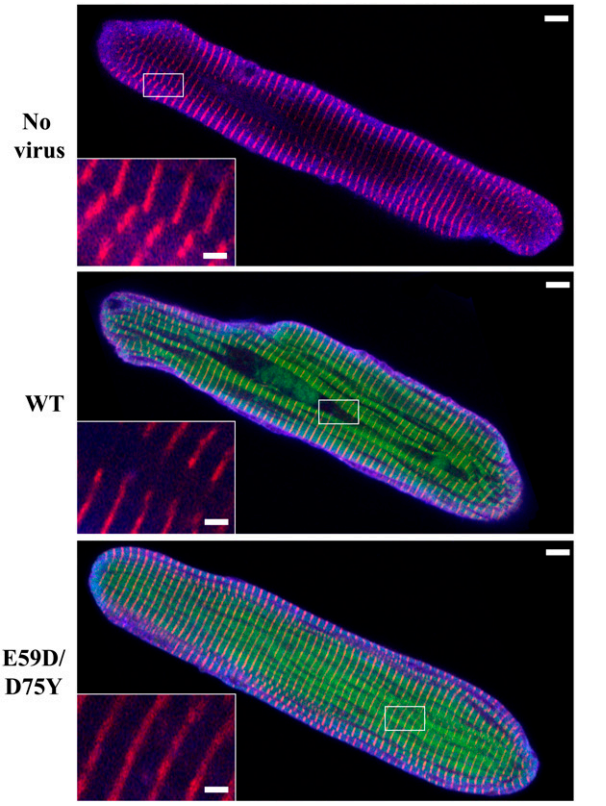

FIGURE 2 Confocal fluorescence images of adenoviral infected cardiomyocytes. Intact cells were fixed and double labeled with an antibody to TnC (*cyan*) and the Z-line protein α-actinin (*red*). Myocytes infected with adenovirus have, in addition, a green fluorescence due to coexpression of GFP (for comparison, GFP fluorescence was removed in the insets). The α-actinin staining of the Z-lines exhibits a clear periodic pattern characteristic of striated muscle, with TnC staining between the Z-lines. The bar at lower magnification is 5 μm and the bar in the inset is 1 μm.

We used confocal microscopy to examine if exogenous TnC incorporation into the myofilaments altered sarcomere ultra-structure (Fig. 2). Noninfected myocytes and myocytes infected with WT and $TnC^{(E59D,D75Y)}$ adenovirus (confirmed by GFP fluorescence) exhibit a periodic Z-line immunostaining pattern of α-actinin (red fluorescence), which is characteristic of all striated muscle. As expected, the TnC antibody decorated the thin filaments as shown by immunofluorescence between the Z-lines (cyan fluorescence). Confocal images for myocytes infected with E59D and D75Y TnC showed similar Z-line and TnC staining patterns (data not shown). These data suggest that exogenous incorporation of TnC into the sarcomere (1) does not alter myofilament stoichiometry, and (2) has no effect on the structural integrity of the sarcomere.

Mutation D75Y impairs cell function without affecting calcium transients

To investigate the physiological relevance of $TnC^{(E59D,D75Y)}$ incorporation into myofilaments, contractility and intracellular calcium transients were measured in intact, electrically stimulated cardiomyocytes. Co-expression of GFP facilitated the identification of myocytes expressing recombinant TnC. The fluorescent properties of GFP, however, complicate the measurement of intracellular calcium indicator, fura-2, due to spectral overlap (34). To circumvent this problem, we titrated our infection protocol to yield a comparable level of GFP expression in the WT and mutant TnC groups (Fig. 1 *A*). In addition, myocytes with similar GFP fluorescence (Materials and Methods) were selected to further minimize the chance of unequal GFP expression between myocytes. This strategy allowed us to differentiate between the functional consequences of mutant TnC expression in the myocytes while accounting for the influence of GFP expression. We found no difference in % cell shortening (CS) between WT and lacZ-GFP infected myocytes (WT = 3.2 ± 0.4% vs. lacZ = 3.5 ± 0.5%). Fig. 3 *A* shows typical tracings of CS and the intracellular calcium transient from WT and E59D/D75Y TnC myocytes, paced at a rate of 3 Hz and maintained at 37°C. The results for %CS and the fura-2 ratio are shown in Fig. 3 *B*. Expression of $TnC^{(E59D,D75Y)}$ resulted in a significant reduction of %CS compared to WT ($TnC^{(E59D,D75Y)}$ =1.5 ± 0.2% vs. WT = 3.2 ± 0.4%; $p < 0.0001$). The decrease in %CS observed in TnC^{D75Y} was comparable to that seen in $TnC^{(E59D,D75Y)}$ (TnC^{D75Y} = 1.5 ± 0.2%; $p < 0.0005$ vs. WT), whereas mutation E59D had no effect (TnC^{E59D} = 2.9 ±

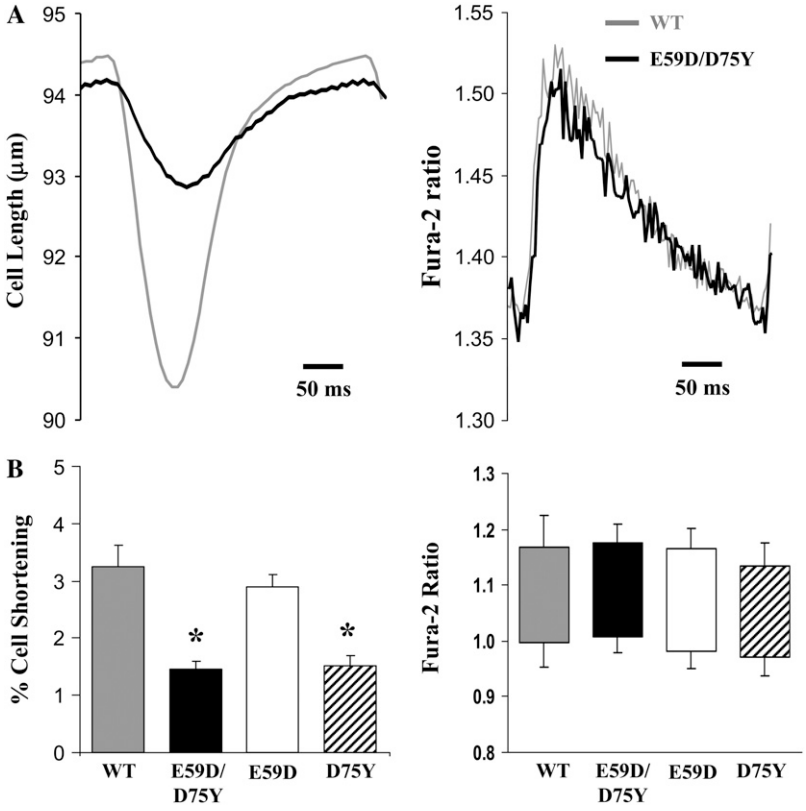

FIGURE 3 Cell shortening and calcium transients in intact myocytes at 4 days post-adenoviral infection. (*A*) Representative cell shortening and fura-2 calcium transients of WT (*black*) and $TnC^{(E59D,D75Y)}$ (*gray*) cardiomyocytes. (*B*) Bar graphs showing results for % cell shortening and fura-2 ratio (systolic is top and diastolic is bottom of floating bar). Cell shortening in $TnC^{(E59D,D75Y)}$ (*black*, $n = 28$) and TnC^{D75Y} (*cross-hatched*, $n = 27$) myocytes were decreased significantly compared to WT (*gray*, $n = 22$) or TnC^{E59D} (*white*, $n = 29$), whereas intracellular calcium was not different between the groups. Data expressed as mean ± SE. $*p < 0.05$ $TnC^{(E59D,D75Y)}$ and TnC^{D75Y} versus WT and TnC^{E59D} by one-way ANOVA, Newman-Keuls post-hoc test.

0.2%; p = NS vs. WT). Interestingly, the observed differences were Ca^{2+}-independent, because the fura-2 ratio transients were similar among all groups. These data suggest that impairment of contractility in $TnC^{(E59D,D75Y)}$ cells is at the level of the myofilaments, as the intracellular calcium transient was unaffected, and that the functional impairment is mediated by mutation D75Y.

Mutation D75Y decreases myofilament calcium responsiveness in permeabilized cells

Co-expression of GFP allowed for easy identification of adenoviral infected cells that were used subsequently for measurement of myofilament calcium responsiveness. To directly assess the state of the myofilament contractile apparatus, selected myocytes were Triton-permeabilized and the contractile response (SL shortening) of the skinned myocyte to various calcium concentrations was determined, as described previously (17). There was no difference in resting SL at pCa9 between the groups (WT = 1.818 ± 0.003, $TnC^{(E59D,D75Y)} = 1.827 \pm 0.006$, $TnC^{E59D} = 1.825 \pm 0.005$, $TnC^{D75Y} = 1.818 \pm 0.04$; p = NS). Fig. 4 *A* shows representative SL tracings from WT and $TnC^{(E59D,D75Y)}$ cells exposed to increasing calcium solutions, and Fig. 4 *B* shows the relationship between the maximum SL change versus pCa. The SL-pCa curves for noninfected cells, and cells infected with lacZ-GFP were not different from WT (data not shown). Incorporation of $TnC^{(E59D,D75Y)}$ resulted in marked depression of myofilament calcium responsiveness at high $[Ca^{2+}]$ when compared to WT. Similar to the myocyte contractility data, results from the single mutants showed that the decrease in myofilament calcium responsiveness in TnC^{D75Y} is almost identical to that observed in $TnC^{(E59D,D75Y)}$, whereas TnC^{E59D} was not different from WT control. These data suggest that the impaired myofilament calcium responsiveness in permeabilized $TnC^{(E59D,D75Y)}$ myocytes is mediated by mutation D75Y.

Myofilament calcium sensitivity is decreased in rabbit psoas fibers reconstituted with mutant TnC

The cell shortening-pCa assay does not control for sarcomere length, which is an important determinant of myofilament calcium sensitivity. Thus, to unequivocally address whether the observed contractile phenotypes were due to a decrease in myofilament calcium sensitivity, we measured the force-pCa relationship in rabbit psoas fibers reconstituted with recombinant TnC. Endogenous skeletal TnC was extracted from membrane permeabilized, fixed-end (sarcomere length ~2.5 μm), psoas fibers, and reconstituted with either purified native sTnC, WT cTnC, or $TnC^{(E59D,D75Y)}$. SDS-PAGE analysis of myofibril extracts confirmed that only TnC was affected by the extraction/reconstitution procedure (Fig. 5 *A*). Endogenous TnC extraction was verified by a reduction in force at pCa 4.0 to <2% of the pre-extraction value (Fig. 5 *B*).

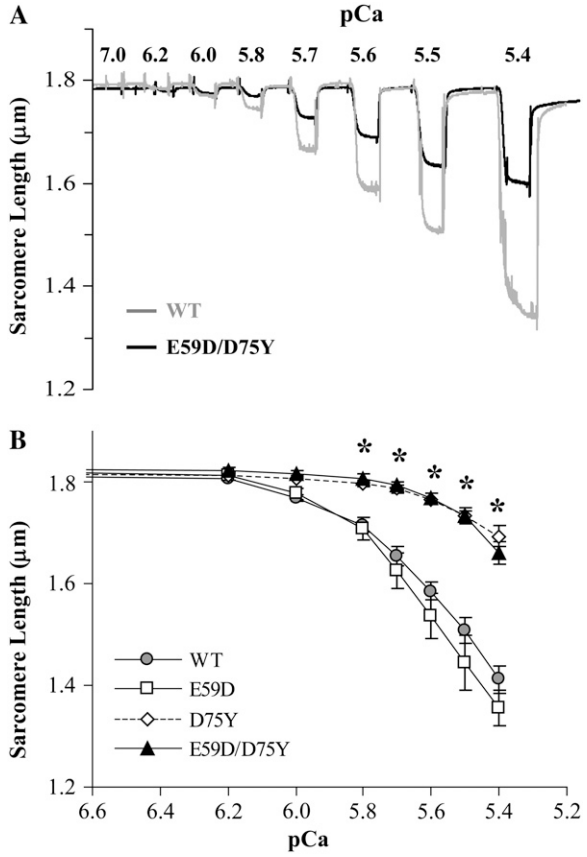

FIGURE 4 Myofilament calcium responsiveness in permeabilized myocytes at 4 days post-adenoviral infection. (*A*) Representative tracings of sarcomere shortening in WT and $TnC^{(E59D,D75Y)}$ myocytes induced by a stepwise increase in calcium concentration, expressed as pCa. After each pCa solution change, the skinned myocyte was reperfused with relaxing solution (pCa 9) until recovery of slack sarcomere length was obtained. (*B*) The sarcomere length change-pCa relationships of WT and mutant TnC infected cardiomyocytes. The myofilament calcium responsiveness of $TnC^{(E59D,D75Y)}$ (*triangle*, $n = 9$) and TnC^{D75Y} (*diamond*, $n = 11$) myocytes was markedly blunted compared to WT (*circle*, $n = 9$) or TnC^{E59D} (*square*, $n = 9$). Data expressed as mean ± SE. $*p < 0.05$ $TnC^{(E59D,D75Y)}$ and TnC^{D75Y} versus WT and TnC^{E59D} by two-way ANOVA, Bonferroni post-hoc test.

Reconstitution with WT cTnC resulted in ~40% decrease in maximal force when compared to fibers reconstituted with native sTnC (Fig. 5 *C*). This is similar to what was reported previously (35,36), and may simply reflect differences in the interaction between cTnC and skeletal TnI and TnT as previously suggested (37). Reconstitution with $TnC^{(E59D,D75Y)}$ resulted in an even greater decrease in maximal force, ~75% compared to sTnC (~50% compared to reconstituted WT cTnC). The force-pCa relations were normalized and fitted to a general Hill equation. In Fig. 6 *A*, $TnC^{(E59D,D75Y)}$ exhibited a decrease in myofilament calcium sensitivity as shown by a rightward shift of the force-pCa curve relative to WT cTnC ($pCa_{50} = 5.9 \pm 0.10$ vs. $pCa_{50} = 6.2 \pm 0.04$; $p < 0.05$). There was no significant difference in myofilament cooperativity as judged by the Hill coefficient ($n = 1.8 \pm 0.8$ vs. $n = 1.9 \pm 0.07$; p = NS).

Calcium binding affinity is decreased in mutant TnC

We postulated that the observed contractile phenotypes were directly attributable to mutation D75Y, which is located in the regulatory Ca^{2+}-binding pocket II and thus was predicted to alter TnC Ca^{2+}-binding affinity. TnC Ca^{2+} binding affinity was derived from Ca^{2+} titration curves by measuring the Ca^{2+}-induced increase in fluorescence intensity in IAANS-labeled TnC. The fluorescence-pCa relationships were fitted to a general Hill equation. In Fig. 6 *B*, $TnC^{(E59D,D75Y)}$ again exhibited a rightward shift of the fluorescence-pCa curve relative to WT cTnC, indicative of a decrease in Ca^{2+} binding affinity ($pCa_{50} = 5.0 \pm 0.10$ vs. $pCa_{50} = 5.4 \pm 0.05$ $p < 0.05$).

D75Y mutation decreases functional concerted motions in cNTnC

To further elucidate a detailed molecular mechanism underlying the reduced Ca^{2+}-binding affinity associated with mutation D75Y, we carried out molecular dynamics (MD) simulations on cNTnC (PDB entry: 1SPY) (22). Mutant E59D was functionally irrelevant and was not included in the computational analyses. The Asp75 → Tyr mutation removes negative charge, and was therefore expected to alter the electrostatic interaction of the cNTnC structure. Interestingly, the mutation also caused the side-chain of Tyr75 to point toward helix N, and formed a van der Waals interaction with Val9 (Fig. 7). The favorable van der Waals interaction between Tyr75 and helix N is approximately −3.3 kcal/mol averaged along the MD trajectories, compared with less than −0.5 kcal/mol for the WT. MD simulations on the WT and mutant D75Y showed no significant differences in root mean-square deviation from the initial structure (Fig. 8 *A*). Structural analysis along the MD trajectory also showed no significant differences in secondary structure fluctuations, except for helix N in mutant D75Y that seemed to be more stable due presumably to the van der Waals contact between Val9 and Tyr75 (Fig. 8 *B*).

From the normal mode analysis, we obtained the concerted motions between the residues of the cNTnC structure. Concerted motions provide information on the regions within a molecule that move in a correlated or anti-correlated manner, and thus offer a more detailed accounting of conformational changes important for protein function. WT cNTnC (Fig. 9 *A*) exhibited significant concerted motions, notably anti-correlated motions (−0.4 to −1.0) between the helix A–β1 loop (residues 25–32, Ca^{2+}-binding Site I) and the anti-parallel β-sheet (β1: 35–37 and β2: 71–73), correlated motions between the two strands of the β-sheet, as well as between the helix C–β2 loop (Ca^{2+}-binding Site II) and β1–helix B loop. Importantly, the regulatory Ca^{2+}-binding loop II (residues 65–76) seems to be an active region for concerted motions (Fig. 9 *A*). These concerted motions are considerably reduced in the mutant D75Y (Fig. 9 *B*), suggesting an important role

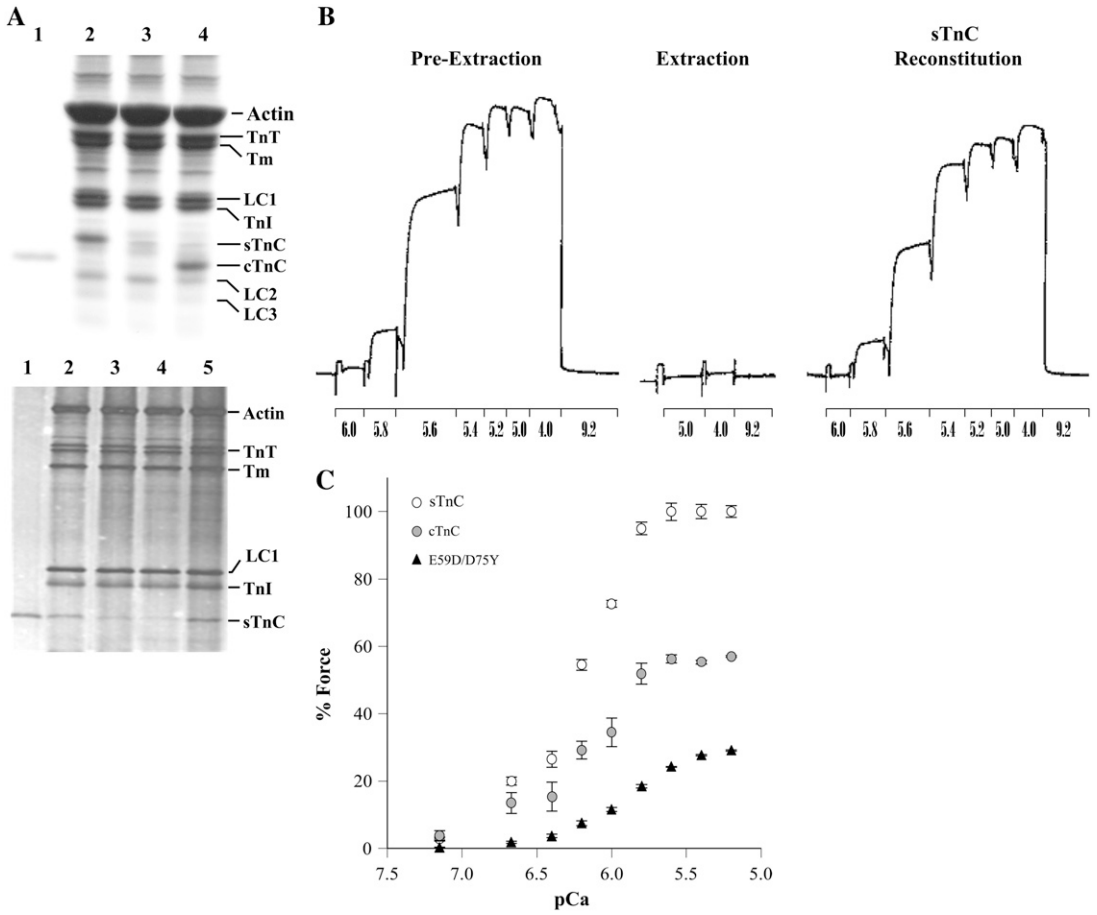

FIGURE 5 TnC extraction and reconstitution in rabbit psoas fibers and force-pCa measurement. (*A*) Rabbit psoas fiber extracts before and after TnC replacement were subjected to SDS-PAGE analysis. (*Upper panel*) 4–20% gel was stained with Coomassie, (*lane 1*) Purified cTnC, (*lane 2*) untreated control, (*lane 3*) 12 min TnC extraction, (*lane 4*) 10 min reconstitution with cTnC (note: cTnC migrates ahead of sTnC). (*Lower panel*) 12.5% gel was silver-stained, (*lane 1*) purified sTnC, (*lane 2*) 10 min reconstitution with sTnC, (*lane 3*) 5 min reconstitution with sTnC, (*lane 4*) 12 min TnC extraction, (*lane 5*) untreated control. TnT, troponin T; Tm, tropomyosin; TnI, troponin I; sTnC, skeletal TnC; cTnC, cardiac TnC; LC1, LC2, and LC3 are myosin light chains 1, 2, and 3, respectively. (*B*) Representative chart recording of force in a single skinned rabbit psoas fiber at various pCa solutions before endogenous sTnC extraction, after extraction, and after reconstitution with native sTnC. The pCa values of the solutions are shown below the tracings. (*C*) The force-pCa relationships were obtained from skinned rabbit psoas fibers after reconstitution with either native sTnC (*open circle*, $n = 6$), WT cTnC (*gray circle*, $n = 8$), or mutant $TnC^{(E59D,\ D75Y)}$ (*black triangle*, $n = 8$). All data were normalized to the average force value obtained at pCa 4.0 with sTnC reconstitution and the data expressed as mean ± SE.

for concerted motions in loop II for Ca^{2+}-binding affinity. Although we do not know the precise mechanism, one possible explanation is that the van der Waals interaction between Val9 and Tyr75 in the mutant sterically hinders the motion of the β-sheet as well as its upstream and/or downstream loops including the Ca^{2+}-binding loop. We take these data as evidence that a decrease in concerted motions in the calcium regulatory domain of TnC directly interferes with the calcium binding properties of TnC.

DISCUSSION

In this report, we describe functional and structural consequences of two novel missense mutations in cardiac TnC isolated from a patient diagnosed with idiopathic dilated cardiomyopathy. We found that cardiomyocytes expressing mutation D75Y, but not E59D, in TnC exhibited impaired myocyte contractility, despite normal calcium transients, and decreased myofilament calcium sensitivity. At the protein level, Ca^{2+}-binding affinity was decreased in mutant TnC and this is consistent with our computational analysis that show a dramatic decrease in intramolecular concerted motions in the regulatory Ca^{2+}-binding pocket of TnC. Our study provides mechanistic insight into how a specific mutation directly alters the dynamic molecular microenvironment in TnC leading to impairment of myofilament calcium signal transmission with consequent cardiomyocyte contractile dysfunction.

Functional effects of $TnC^{(E59D,D75Y)}$

Mutation D75Y, located in the regulatory Ca^{2+}-binding Site II, is juxtaposed to the last calcium coordinating position and

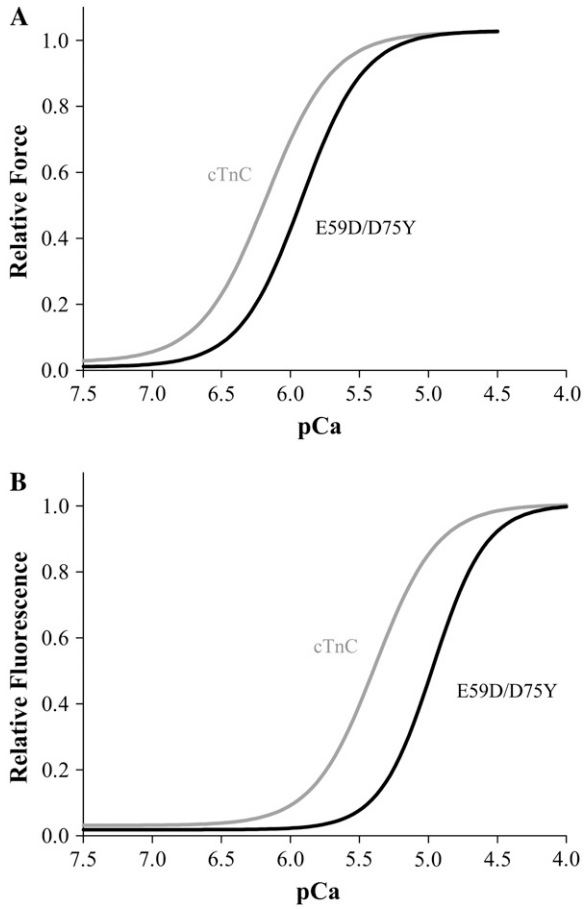

FIGURE 6 Force-pCa and fluorescence-pCa relationships. (*A*) Force-pCa data after TnC reconstitution were normalized to the force obtained at pCa 4.0 and a modified Hill equation (see Materials and Methods) was fitted to the data. (*B*) Fluorescence of IAANS-labeled recombinant TnC was titrated with Ca^{2+}. The data was normalized to the fluorescence obtained at pCa 4.0, and the Hill equation was fitted to the data. The fitted curves for the mean data are shown, WT cTnC (*gray*) and mutant $TnC^{(E59D,D75Y)}$ (*black*).

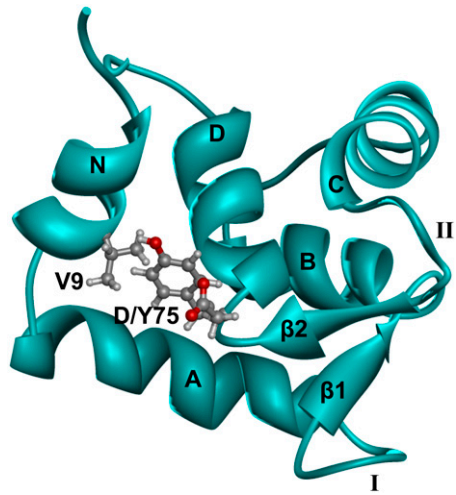

FIGURE 7 Structure of the N terminus of cardiac TnC (PDB entry: 1SPY). The helices of TnC are labeled N and A–D and the β-strands are labeled β1 and β2. Val9 and D/Y75 are shown explicitly using the ball-and-stick model (color scheme is: C in *gray*, H in *white*, and O in *red*). The mean minimum heavy-atom distance between D75 and V9 was ~6 Å in the WT cNTnC simulation, whereas the distance dropped to 4.2 Å between Y75 and V9 in the simulation of the mutant. The two Ca^{2+}-binding sites are labeled as Site I and Site II. In the Ca^{2+}-saturated form, Ca^{2+} binds to Site II whereas Site I is empty.

thus was expected to interfere with normal calcium binding of the coordinating residues. Mutation E59D is located in the proximal helix flanking loop II (helix C), which has been suggested to be important in ''fine tuning'' of calcium binding to the regulatory site of TnC, as site-directed mutagenesis of helix C in skeletal TnC was shown to decrease calcium binding affinity (38). To determine the functional effects of $TnC^{(E59D,D75Y)}$, as well as the individual TnC mutations, we incorporated the TnC mutants into cardiac myocytes, using the adenoviral methodology that has been shown previously to be an efficient assay for robust incorporation of other recombinant myofilament proteins TnI, TnT, and tropomyosin in cardiomyocytes (32,39,40). Importantly, our assay resulted in targeted remodeling of TnC in the troponin complex, without any alteration in the composition of other myofilament proteins or ultra-structural changes in the sarcomeric lattice. Under these conditions, we found a consistent and striking functional phenotype caused by $TnC^{(E59D,D75Y)}$ with impaired cell contractility and impaired myofilament calcium responsiveness in intact and permeabilized cells, respectively. Furthermore, the impaired $TnC^{(E59D,D75Y)}$ phenotype was completely recapitulated by mutation D75Y, whereas E59D seemed to be functionally benign. The fact that intracellular calcium homeostasis was not different between WT and mutant TnC groups, clearly points to a defect at the level of the myofilaments, which was confirmed in our force-pCa experiments showing a decrease in myofilament Ca^{2+}-sensitivity in fixed-end psoas fibers reconstituted with $TnC^{(E59D,D75Y)}$. We further go on to show that the ability of the mutant TnC to bind Ca^{2+} is altered as Ca^{2+}-binding affinity in IAANS-labeled recombinant $TnC^{(E59D,D75Y)}$ was decreased. An important aspect in considering intracellular calcium homeostasis is the rapid buffering of cytosolic calcium that is mediated in large part by TnC (~60% of total cytoplasmic calcium buffering capacity) (41). A decrease in $TnC^{(E59D,D75Y)}$ calcium binding affinity is expected to affect the rapid cytoplasmic calcium buffering capacity that, in turn, could affect the intracellular calcium transient, provided the calcium flux through the sarcoplasmic reticulum (SR) and sarcolemma remain unchanged. Intracellular calcium homeostasis, however, was unaffected by either $TnC^{(E59D,D75Y)}$ or TnC^{D75Y} incorporation into the myofilaments, suggesting that normal calcium cycling was maintained despite altered $TnC^{(E59D,D75Y)}$ calcium binding/buffering. Further studies are needed to determine whether normal calcium homeostasis was maintained as a result of

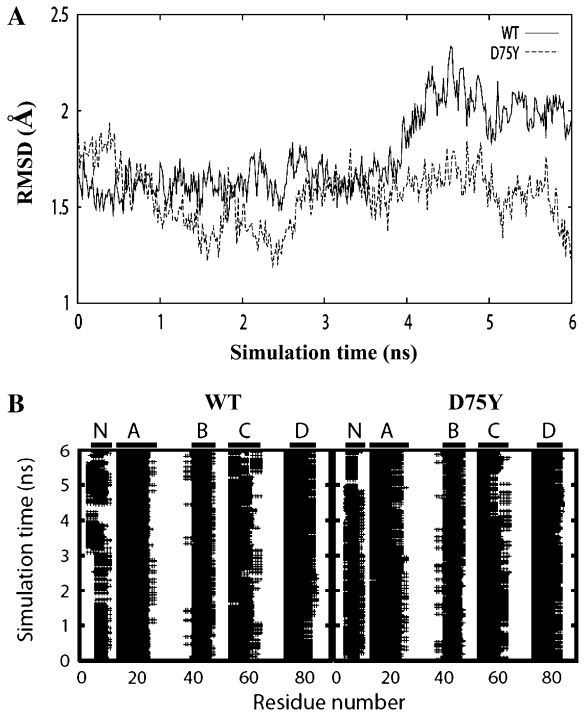

FIGURE 8 Computational analysis of the Ca^{2+}-free form of cNTnC. (*A*) Root mean-square deviation (RMSD) showed relatively stable structures for both WT and mutant D75Y. (*B*) Secondary structure analysis along the molecular dynamics trajectory of Ca^{2+}-free cNTnC. The secondary structure assignment of helices N and A–D are labeled at the top of the graphs. A plus sign denotes the helical conformation, whereas the blank spaces represent nonhelical conformations. Results for WT (*left panel*) and mutant D75Y (*right panel*) show similarity between the helical conformations except that helix N is more stable in mutant D75Y.

compensatory changes in other calcium-handling proteins (e.g., Na^+/Ca^{2+} exchanger, SR Ca^{2+}-ATPase, ryanodine receptors) to offset the decrease in $TnC^{(E59D,D75Y)}$ calcium binding and/or buffering. Taken together, our findings show a clear functional deficit in $TnC^{(E59D,D75Y)}$ and TnC^{D75Y} myocytes that was independent of intracellular calcium levels and occurred at the level of the mutant TnC.

Molecular basis of TnC^{D75Y} phenotype

It is well documented that in skeletal TnC, the regulatory N domain switches from a ''closed'' to ''open'' state on binding of two calcium ions, causing helices N, A, and D to move as a unit away from helices B and C. This conformational switch exposes a hydrophobic cleft in TnC for binding of skeletal TnI. By contrast, binding of calcium in the N-terminus of cardiac TnC (cNTnC) causes minimal conformational change, and studies have shown that binding of a C-terminal fragment of cardiac TnI (in a region spanning residues 147–163) in the hydrophobic cleft is needed to induce the fully ''open'' state in cNTnC (7,8). The canonical motif in Ca^{2+}-binding proteins that permits Ca^{2+} coordination is the EF-hand (helix–loop–helix), with the 12-residue loop containing three negatively charged acid pairs at positions 1 ($+x$) and 9 ($-x$), 3 ($+y$) and 7 ($-y$) and 5 ($+z$) and 12 ($-z$) that bind Ca^{2+} (10). The acid pairs form a quasi-planar pentagon structure that coordinate Ca^{2+} and mutational analysis of the EF-hand protein, calmodulin, has shown that the acid pairs increase Ca^{2+} affinity by increasing the rate of Ca^{2+} association (42). In our study, the D75Y mutation, juxtaposed to the $-z$ coordinating position, removes a negatively charged residue from Ca^{2+}-binding Site II and this change in electrostatic long-range interaction could alter the kinetics of Ca^{2+}-exchange. Decreasing the negative charge in the Ca^{2+}-binding loop by replacement of the Asp75 with Tyr is expected to decrease the Ca^{2+} association rate, even if the residue is not in a Ca^{2+} coordinating position, leading ultimately to decreased TnC Ca^{2+} affinity as observed for the D75Y mutant. Thus, mutation D75Y may have induced a structural modification in the regulatory ''closed'' domain of TnC that could have obstructed calcium binding, thus resulting in a diminished trigger for initiating actin-myosin interaction at any given calcium concentration. To further address this central question, we carried out molecular dynamics simulations using the published Ca^{2+}-free TnC structure (22). It should be noted that although there have been extensive studies on the static structure and biochemical properties of TnC, no study has looked at the dynamic correlated motions of this protein. Subject to limitations in sampling time and computational molecular approximations, molecular dynamics has been shown to provide detailed information regarding conformational changes in a protein. Our analysis showed that even though the mutant Tyr75 residue did not seem to directly interfere with calcium coordination as it was pointed away from the Ca^{2+}-binding pocket, it introduced a new hydrophobic interaction between Tyr75 and Val9 not present in the wild-type (Fig. 7). Interestingly, our simulations showed no obvious global structural perturbations with the introduction of Tyr75 in TnC. Analysis of concerted motions showed the presence of correlated and anti-correlated motions in Ca^{2+}-binding Site II of WT TnC that were reduced significantly by the D75Y mutation. We interpret this as evidence that the molecular concerted motions of cNTnC (greatly facilitated by the negative Asp75 charge of the loop), is important in establishing the Ca^{2+} binding kinetics of cTnC. Removal of the negative charge and/or introduction of the Tyr75/Val9 hydrophobic interaction in the D75Y mutant reduces the extent of concerted motions in cNTnC, which we predict will interfere with the Ca^{2+} on-rate, and thus impair Ca^{2+} binding affinity. Lehrer and Geeves (43) and McKillop and Geeves (44) have proposed a three-state model for thin filament activation and suggested that Ca^{2+} binding to TnC shifts the equilibrium of thin filament states from the 'blocked' to the 'closed' state, and the development of strong crossbridges further shifting the 'closed' to the 'open' state. In this context, our results would suggest that mutant D75Y limits the transition from

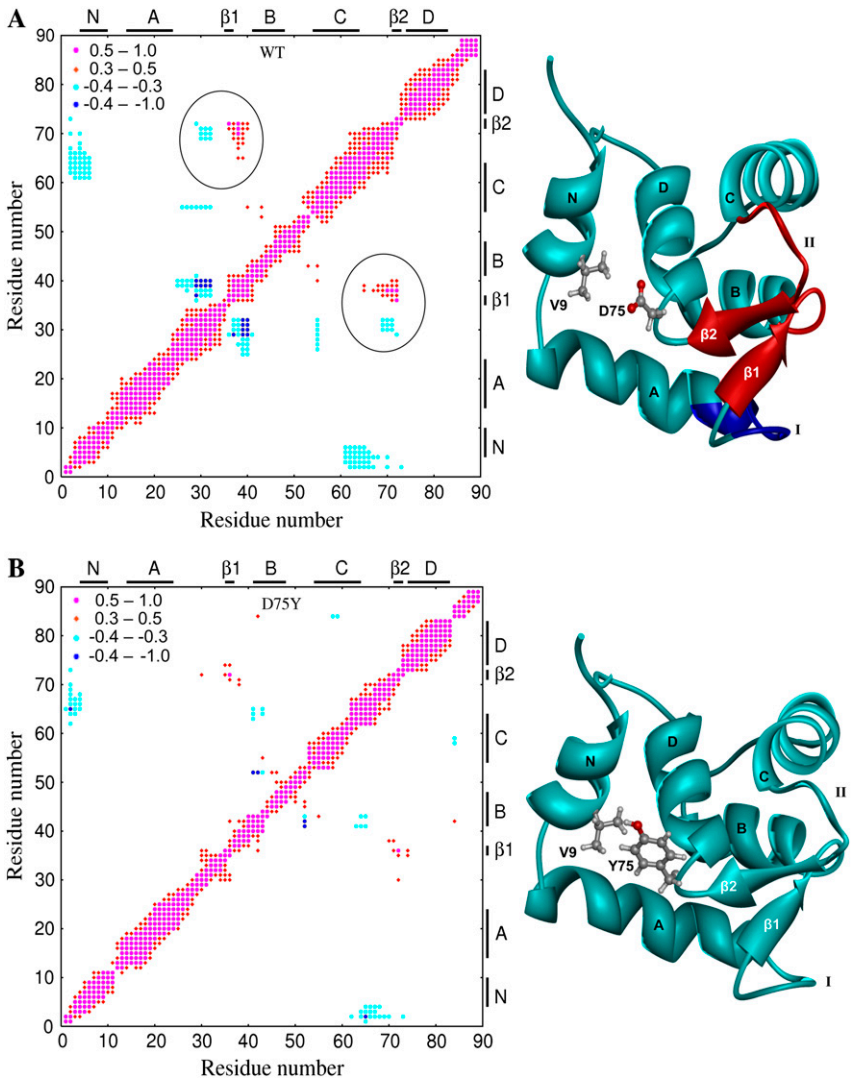

FIGURE 9 Concerted motions calculated from the 500 largest vibrational modes from WT and mutant Ca^{2+}-free cNTnC. The secondary structure assignment is labeled at the top and side. Residues within the same helical region have the highest correlated motion, as shown by diagonal red dots in both WT and mutant (note the diagonal symmetry of the graphs). (*A*) WT exhibited significant anti-correlated (between the helix A – β1 loop, (residues 25–32) and β-sheet (35–37 and 71–73)) and correlated motions (between the two strands of β-sheet as well as the helix C–β2 loop and the β1–helix B loop). Circle denotes concerted motions in the Ca^{2+}-binding pocket. The corresponding ribbon structure of the WT cTnC (PDB entry: 1SPY) with the off-diagonal mapped concerted motions is shown to the right. The anti-correlated motion is between the blue region (residues 25–32) and the red regions, whereas the correlated motions are between the red regions. (*B*) The extent of concerted motions is dramatically reduced in the D75Y mutant as shown by the secondary structure assignment and the corresponding mutant ribbon structure.

the 'blocked' to the 'closed' state, thereby diminishing the probability of movement to the 'open' state and thus reducing force generation.

Even though our experimental and simulation data strongly suggest an impairment in Ca^{2+}-binding affinity of mutant TnC, bear in mind that TnC does not function in isolation but as part of an integrated contractile system. Both TnI and TnT, and more recently myosin have been shown to influence the Ca^{2+}-binding properties of TnC (5,45). This Ca^{2+}-dependent interplay between TnC and the other myofilament proteins may lead to a mechanism whereby the calcium-bound mutant TnC alters downstream myofilament interactions that in turn ''negatively'' feeds back on TnC Ca^{2+}-binding affinity. Our data, however, seems to dispute this notion as myofilament cooperativity (as judged by the Hill coefficient in the force-pCa experiments) was not altered by mutant TnC. Thus, our results strongly implicate impaired Ca^{2+}-binding affinity of mutant TnC as a primary event in $TnC^{(E59D,D75Y)}$ myocyte contractile dysfunction.

Implications for disease

A growing body of evidence has implicated myofilament mutations as primary causes of myocardial disorders, and mutations in β-myosin heavy chain, troponin T, tropomyosin, actin, and titin have all been associated with familial dilated cardiomyopathy (46). It is important to emphasize that the TnC mutations characterized in the current investigation were identified from left ventricular tissue obtained from a single patient diagnosed with idiopathic dilated cardiomyopathy. Regrettably, it was not possible for us to retrieve the patient's medical records or procure any DNA from the patient for confirmation of the TnC mutations by genotyping. Repeated RNA analyses from different sections of the tissue sample, however, yielded the same result that makes it unlikely that the reported TnC mutations represent cloning artifacts. We also recognize that linkage analyses or co-segregation studies are necessary to fully elucidate whether the mutant TnC characterized in this study is indeed a causal disease gene for dilated cardiomyopathy. Recently, a missense

mutation (G159D) in TnC was identified in a family with inherited dilated cardiomyopathy (47). The mutation was located in the C-terminal lobe of troponin C, considered to be the anchoring domain of TnC to the troponin complex, and showed altered intertroponin interactions, in vitro. Two recent articles scrutinized more closely the G159D TnC mutation and showed that although the force-pCa relationship was unaffected, the mutation decreased the rate of force production in reconstituted skinned fibers (48) and blunted the TnI phosphorylation induced decrease in Ca^{2+}-sensitive tension development (49). These recent reports are significant as they challenge a commonly held notion that myofilament mutations associated with dilated cardiomyopathy converge on a final common pathway leading to reduced myofilament Ca^{2+} sensitivity (50). Whatever the mechanism, our study and those by others, identify TnC as another candidate gene in the growing list of sarcomere gene mutations linked with dilated cardiomyopathy.

SUMMARY AND CONCLUSIONS

Our findings showed a disruption in concerted motions in the regulatory domain of mutant D75Y TnC, which we postulate to be a mechanism underlying the decrease in myofilament calcium sensitivity and impaired contractility in cardiomyocytes expressing mutant TnC. The observed cellular dysfunction in cardiomyocytes expressing mutant D75Y TnC recapitulates many of the dysfunctional features of dilated cardiomyopathy. Although it is not entirely clear how a primary defect in TnC calcium binding affinity leads to aberrant ventricular remodeling, a decrease in systolic function would contribute significantly to compensatory responses in an effort to maintain cardiac output. These include elevated end-diastolic volumes, which result in significant increases in wall stress at any given pressure with adverse consequences for cell survival, triggering a cycle of maladaptive events characterized by progressive ventricular dilatation. Congestive heart failure is often associated with desensitization of the myocardium to calcium. Understanding the molecular mechanisms that regulate TnC calcium binding and signal transmission could therefore lead to the design of calcium sensitizing agents useful in the treatment of heart failure.

We thank the National Center of Supercomputing Applications and the Scientific Computing and Visualization group at Boston University for providing computational resources.

This work was supported by National Institute on Aging (1K01AG024056); American Heart Association (0430087N) (C.C.L.); National Institutes of Health (RR-10888 and RR-15942) (C.E.C.) and (HL-67297, HL-71775 and HL-73756) (R.L.); and National Science Foundation Major Research Instrumentation (DBI-0320875).

REFERENCES

1. Solaro, R. J., and H. M. Rarick. 1998. Troponin and tropomyosin: proteins that switch on and tune in the activity of cardiac myofilaments. *Circ. Res.* 83:471–480.
2. Gordon, A. M., E. Homsher, and M. Regnier. 2000. Regulation of contraction in striated muscle. *Physiol. Rev.* 80:853–924.
3. Parmacek, M. S., and J. M. Leiden. 1991. Structure, function, and regulation of troponin C. *Circulation.* 84:991–1003.
4. Holroyde, M. J., S. P. Robertson, J. D. Johnson, R. J. Solaro, and J. D. Potter. 1980. The calcium and magnesium binding sites on cardiac troponin and their role in the regulation of myofibrillar adenosine triphosphatase. *J. Biol. Chem.* 255:11688–11693.
5. Johnson, J. D., J. H. Collins, S. P. Robertson, and J. D. Potter. 1980. A fluorescent probe study of Ca^{2+} binding to the Ca2+-specific sites of cardiac troponin and troponin C. *J. Biol. Chem.* 255:9635–9640.
6. Calvert, M. J., D. G. Ward, H. R. Trayer, and I. P. Trayer. 2000. The importance of the carboxyl-terminal domain of cardiac troponin C in Ca^{2+} -sensitive muscle regulation. *J. Biol. Chem.* 275:32508–32515.
7. Dong, W. J., J. Xing, M. Villain, M. Hellinger, J. M. Robinson, M. Chandra, R. J. Solaro, P. K. Umeda, and H. C. Cheung. 1999. Conformation of the regulatory domain of cardiac muscle troponin C in its complex with cardiac troponin I. *J. Biol. Chem.* 274:31382–31390.
8. Li, M. X., L. Spyracopoulos, and B. D. Sykes. 1999. Binding of cardiac troponin-I147–163 induces a structural opening in human cardiac troponin-C. *Biochemistry.* 38:8289–8298.
9. Collins, J. H. 1991. Myosin light chains and troponin C: structural and evolutionary relationships revealed by amino acid sequence comparisons. *J. Muscle Res. Cell Motil.* 12:3–25.
10. Strynadka, N. C., and M. N. James. 1989. Crystal structures of the helix-loop-helix calcium-binding proteins. *Annu. Rev. Biochem.* 58: 951–998.
11. Chomczynski, P., and N. Sacchi. 1987. Single-step method of RNA isolation by acid guanidinium thiocyanate-phenol-chloroform extraction. *Anal. Biochem.* 162:156–159.
12. Gahlmann, R., R. Wade, P. Gunning, and L. Kedes. 1988. Differential expression of slow and fast skeletal muscle troponin C. Slow skeletal muscle troponin C is expressed in human fibroblasts. *J. Mol. Biol.* 201:379–391.
13. Nagata, K., C. Communal, C. C. Lim, M. Jain, T. M. Suter, F. R. Eberli, N. Satoh, W. S. Colucci, C. S. Apstein, and R. Liao. 2000. Altered beta-adrenergic signal transduction in nonfailing hypertrophied myocytes from Dahl salt-sensitive rats. *Am. J. Physiol. Heart Circ. Physiol.* 279:H2502–H2508.
14. Lim, C. C., C. S. Apstein, W. S. Colucci, and R. Liao. 2000. Impaired cell shortening and relengthening with increased pacing frequency are intrinsic to the senescent mouse cardiomyocyte. *J. Mol. Cell. Cardiol.* 32:2075–2082.
15. Jensen, O. N., M. Wilm, A. Shevchenko, and M. Mann. 1999. Sample preparation methods for mass spectrometric peptide mapping directly from 2-DE gels. *Methods Mol. Biol.* 112:513–530.
16. Shevchenko, A., M. Wilm, O. Vorm, and M. Mann. 1996. Mass spectrometric sequencing of proteins silver-stained polyacrylamide gels. *Anal. Chem.* 68:850–858.
17. Lim, C. C., M. H. Helmes, D. B. Sawyer, M. Jain, and R. Liao. 2001. High-throughput assessment of calcium sensitivity in skinned cardiac myocytes. *Am. J. Physiol. Heart Circ. Physiol.* 281:H969–H974.
18. Potter, J. D. 1982. Preparation of troponin and its subunits. Meth Enzymol 85:241–263.
19. Gordon, A. M., Y. Qian, Z. Luo, C. K. Wang, R. L. Mondares, and D. A. Martyn. 1997. Characterization of troponin-C interactions in skinned barnacle muscle: comparison with troponin-C from rabbit striated muscle. *J. Muscle Res. Cell Motil.* 18:643–653.
20. Liao, R., and J. K. Gwathmey. 1994. Effects of MCI-154 and caffeine on Ca^{++}-regulated interactions between troponin subunits from bovine heart. *J. Pharmacol. Exp. Ther.* 270:831–839.
21. Heck, H. D. 1971. Statistical theory of cooperative binding to proteins. The Hill equation and the binding potential. *J. Am. Chem. Soc.* 93:23–29.
22. Spyracopoulos, L., M. X. Li, S. K. Sia, S. M. Gagne, M. Chandra, R. J. Solaro, and B. D. Sykes. 1997. Calcium-induced structural transition in

the regulatory domain of human cardiac troponin C. *Biochemistry*. 36:12138–12146.

23. Pearlman, D. A., D. A. Case, J. W. Caldwell, W. S. Ross, T. E. Chatham, S. DeBolt, D. Ferguson, G. Seibel, and P. A. Kollman. 1995. AMBER, a package of computer programs for applying molecular mechanics, normal mode analysis, molecular dynamics and free energy calculations to simulate the structural and energetic properties of molecules. *Comput. Phys. Commun*. 91:1–41.
24. Wang, J. M., P. Cieplak, and P. A. Kollman. 2000. How well does a restrained electrostatic potential (RESP) model perform in calculating conformational energies of organic and biological molecules? *J. Comput. Chem.* 21:1049–1074.
25. Jorgensen, W. L. 1982. Revised TIPS for simulations of liquid water and aqueous solutions. *J. Chem. Phys*. 77:4156–4163.
26. Berendsen, H. J. C., J. P. M. Postma, W. F. van Gusteren, A. DiNola, and J. R. Haak. 1984. Molecular dynamics with coupling to an external bath. *J. Chem. Phys.* 81:3684–3690.
27. Darden, T., D. York, and L. Pedersen. 1993. Particle mesh Ewald: an N·log(N) method for Ewald sums in large systems. *J. Chem. Phys*. 98:10089–10092.
28. Ryckaert, J. P., G. Cicotti, and H. J. C. Berendsen. 1977. Numerical integration of the cartesian equations of motion of a system with constraints: molecular dynamics of n-alkanes. *J. Comput. Phys*. 23: 327–341.
29. Kabsch, W., and C. Sander. 1983. Dictionary of protein secondary structure: pattern recognition of hydrogen-bonded and geometrical features. *Biopolymers*. 22:2577–2637.
30. Micheletti, C., G. Lattanzi, and A. Maritan. 2002. Elastic properties of proteins: insight on the folding process and evolutionary selection of native structures. *J. Mol. Biol*. 321:909–921.
31. Ichiye, T., and M. Karplus. 1991. Collective motions in proteins: a covariance analysis of atomic fluctuations in molecular dynamics and normal mode simulations. *Proteins.* 11:205–217.
32. Michele, D. E., F. P. Albayya, and J. M. Metzger. 1999. Thin filament protein dynamics in fully differentiated adult cardiac myocytes: toward a model of sarcomere maintenance. *J. Cell Biol.* 145:1483–1495.
33. Robbins, J. 2000. Remodeling the cardiac sarcomere using transgenesis. *Annu. Rev. Physiol*. 62:261–287.
34. Berkova, Z., A. P. Morris, and M. K. Estes. 2003. Cytoplasmic calcium measurement in rotavirus enterotoxin-enhanced green fluorescent protein (NSP4-EGFP) expressing cells loaded with Fura-2. *Cell Calcium.* 34:55–68.
35. Hannon, J. D., P. B. Chase, D. A. Martyn, L. L. Huntsman, M. J. Kushmerick, and A. M. Gordon. 1993. Calcium-independent activation of skeletal muscle fibers by a modified form of cardiac troponin C. *Biophys. J.* 64:1632–1637.
36. Moreno-Gonzalez, A., J. Fredlund, and M. Regnier. 2005. Cardiac troponin C (TnC) and a site I skeletal TnC mutant alter Ca^{2+} versus crossbridge contribution to force in rabbit skeletal fibres. *J. Physiol.* 562:873–884.
37. Piroddi, N., C. Tesi, M. A. Pellegrino, L. S. Tobacman, E. Homsher, and C. Poggesi. 2003. Contractile effects of the exchange of cardiac troponin for fast skeletal troponin in rabbit psoas single myofibrils. *J. Physiol.* 552:917–931.
38. Leblanc, L., A. Bennet, and T. Borgford. 2000. Calcium affinity of regulatory sites in skeletal troponin-C is attenuated by N-cap mutations of helix C. *Arch. Biochem. Biophys*. 384:296–304.
39. Rust, E. M., F. P. Albayya, and J. M. Metzger. 1999. Identification of a contractile deficit in adult cardiac myocytes expressing hypertrophic cardiomyopathy-associated mutant troponin T proteins. *J. Clin. Invest.* 103:1459–1467.
40. Westfall, M. V., F. P. Albayya, and J. M. Metzger. 1999. Functional analysis of troponin I regulatory domains in the intact myofilament of adult single cardiac myocytes. *J. Biol. Chem.* 274:22508–22516.
41. Bers, D. M. 2001. Calcium sources and sinks. *In* Excitation-Contraction Coupling and Cardiac Contractile Force. D. M. Bers, editor. Kluwer Academic Publishers, Dordrecht. 39–56.
42. Black, D. J., S. B. Tikunova, J. D. Johnson, and J. P. Davis. 2000. Acid pairs increase the N-terminal Ca2+ affinity of CaM by increasing the rate of Ca^{2+} association. *Biochemistry*. 39:13831–13837.
43. Lehrer, S. S., and M. A. Geeves. 1998. The muscle thin filament as a classical cooperative/allosteric regulatory system. *J. Mol. Biol*. 277: 1081–1089.
44. McKillop, D. F., and M. A. Geeves. 1993. Regulation of the interaction between actin and myosin subfragment 1: evidence for three states of the thin filament. *Biophys. J*. 65:693–701.
45. Davis, J. P., C. Norman, T. Kobayashi, R. J. Solaro, D. R. Swartz, and S. B. Tikunova. 2007. Effects of thin and thick filament proteins on calcium binding and exchange with cardiac troponin C. *Biophys. J*. 92: 3195–3206.
46. Fatkin, D., and R. M. Graham. 2002. Molecular mechanisms of inherited cardiomyopathies. *Physiol. Rev*. 82:945–980.
47. Mogensen, J., R. T. Murphy, T. Shaw, A. Bahl, C. Redwood, H. Watkins, M. Burke, P. M. Elliott, and W. J. McKenna. 2004. Severe disease expression of cardiac troponin C and T mutations in patients with idiopathic dilated cardiomyopathy. *J. Am. Coll. Cardiol*. 44:2033–2040.
48. Preston, L. C., S. Lipscomb, P. Robinson, J. Mogensen, W. J. McKenna, H. Watkins, C. C. Ashley, and C. S. Redwood. 2007. Functional effects of the DCM mutant Gly159Asp troponin C in skinned muscle fibres. *Pflugers Arch*. 453:771–776.
49. Biesiadecki, B. J., T. Kobayashi, J. S. Walker, R. John Solaro, and P. P. de Tombe. 2007. The troponin C G159D mutation blunts myofilament desensitization induced by troponin I Ser23/24 phosphorylation. *Circ. Res.* 100:1486–1493.
50. Mirza, M., S. Marston, R. Willott, C. Ashley, J. Mogensen, W. McKenna, P. Robinson, C. Redwood, and H. Watkins. 2005. Dilated cardiomyopathy mutations in three thin filament regulatory proteins result in a common functional phenotype. *J. Biol. Chem*. 280:28498–28506.